J. Biomechanics, 1973, Vol. 6, pp. 511–520. Pergamon Press. Printed in Great Britain

PHOTOELASTIC AND FINITE ELEMENT STRESS ANALYSIS OF A RESTORED AXISYMMETRIC FIRST MOLAR*

J. W. FARAH†, R. G. CRAIG‡ and D. L. SIKARSKIE§
University of Michigan School of Dentistry and School of Engineering, Ann Arbor, Michigan 48104, U.S.A.

Abstract—First molars with full gold crown preparations and a shoulder geometry were idealized by an axisymmetric model and analyzed by the photoelastic, as well as the finite element method. The photoelastic model was constructed in two pieces, the restoration and the tooth with the preparation. The two pieces were then luted together and the model was loaded axisymmetrically with 100 lb; it was stress frozen, sliced, and analyzed with the help of a polariscope. The finite element model was subdivided into 348 elements. The radial and axial stresses were plotted as a function of the radius along various horizontal planes in the model. The maximum shear stresses calculated by the finite element method were compared to those obtained by the photoelastic method, and they were found to compare favorably.

EXPERIMENTAL stress analysis of dental structures has been a topic of interest over the past quarter century. The object of such research was the determination and improvement of the mechanical strength of these structures. The photoelastic method, a well recognized engineering technique of stress analysis, first appeared in dental research with the publication by Noonan (1949). Noonan's models were made of Bakelite, with the cavities packed with silver amalgam. A 55 lb load was applied to the center of the restoration. He found that: (a) a flat floor exhibited less stress concentration than the rounded one, and (b) retention points should not be sharp, but rounded to decrease stress concentration.

Haskins, Haack and Ireland (1954) studied the effects of rounding axio-pulpal line angles, as well as the stress distribution associated with the variations of vertical axial walls. They noticed that there was a marked reduction of stress when the pulpal wall was rounded and sloped. Walton and Leven (1955) presented a three-dimensional photoelastic study of an anterior jacket crown. Four models were analyzed and they concluded that the thicker the walls of the jacket, the greater its strength. They also found that maximum mesiodistal width of the preparation was important. Mahler and Peyton (1955) reviewed the general applications of photoelasticity as a research technique for analyzing stresses in dental structures.

Mahler (1956) published his findings of a disto-occlusal restoration in a primary mandibular first molar. He found that the stresses in the restoration in the region of the isthmus were tensile in nature. He also found that the sloping pulpal floor and the beveled pulpal floor exhibited less adverse stress than the flat pulpal floor.

A study of strain patterns in jacket crowns on anterior teeth was published by Lehman and Hampson (1962) in England. They pointed out the effects of leaving rough surfaces on the prepared tooth and the

*Received 11 September 1972.
†Research Associate, Department of Dental Materials, School of Dentistry.
‡Professor and Chairman, Department of Dental Materials, School of Dentistry.
§Associate Professor, Aerospace Engineering Department, School of Engineering.

importance of trying to insure that the porcelain was well condensed and free from voids.

Colin, Kaufman and Paprino (1963) investigated stress concentrations in full crown preparations, and they found that sharp angles at the gingival shoulders ought to be avoided, since such areas were more prone to failure than restorations with rounded line angles.

Johnson (1965) showed that the inclusion of irregularly shaped pulp chambers in three-dimensional photoelastic models of lower molars did not affect the stress distribution in the model, but did change the stress distribution at the base of the cavity. Johnson, Castaldi, Gau and Wysocki (1968) used three-dimensional photoelastic stress analysis to investigate the design of Class I cavity preparations. The models were made of epoxy resin, and they were tested using the frozen stress technique. They remarked that significant stresses existed in planes remote from points of loading, and that rounding internal line angles reduced the stresses significantly.

Craig, El-Ebrashi and Peyton (1967a, b) using two-dimensional photoelasticity, examined several sections of teeth which had inlays and crowns and concluded among other things that compressive stresses could be reduced near the pulpal floor of some cavities, if the load was moved mesially or distally. El-Ebrashi, Craig and Peyton (1969a, b, c, d and 1970) investigated the effects of modifying the geometry in dental restorations. Some of the geometrical variations they studied were: (a) the proximal margins, (b) the parallelism of axial walls, and (c) the amount of occlusal reduction and pins.

Another method of stress analysis which was originally developed (Turner *et al.* 1956) in the aircraft industry is the finite element method. This technique has since seen widespread use not only in aerospace engineering, but also in civil engineering. The finite element method has proven to be extremely effective for the treatment of problems of plane stress and plane strain (Clough, 1960; Clough and Wilson, 1963).

Impressive results were obtained by Grafton and Strome (1963) in the analysis of axisymmetric shells approximated by a series of truncated cone elements. Argyris (1965) made a broad generalization of the matrix displacement technique for analyzing three-dimensional elastic media for both small and large displacement ranges. The body was approximated by an assembly of tetrahedrons for which a simplefied kinematic pattern was prescribed. Ping and Pian (1967) showed theoretically the conditions that would be sufficient to insure a finite element displacement analysis to converge to the exact displacement solution when the size of the elements was progressively reduced.

Although the general concept is applicable to the analysis of three-dimensional solids, most investigations in that area have been made in the field of civil engineering (Rashid and Rockenhauser, 1968; Argyris and Redshaw, 1968 and Ergatoudis *et al.*, 1968). Another class of problems which is of considerable practical interest is the axisymmetric problem under axisymmetric loading. Zienkiewiez (1971), in his book on finite elements, gave an account of the thermal stresses generated in a reactor pressure vessel.

In this study, both the photoelastic, as well as the finite element methods, are used to study the stress distribution in an idealized axisymmetric first molar with a full crown preparation. Both methods have some advantages that will be discussed. Also, the justification for using an axisymmetric model to approximate the first molar will be given in the discussion portion of this report.

MATERIALS AND METHODS

A. *The photoelastic model*

The photoelastic material used was a two component material, an expoxy resin, Epon

828*, and an amine hardener, Jeffamine D400†, mixed in the ratio of 2:1. Once the desired quantity of resin and hardener was established, the components were gently and thoroughly mixed at room temperature so as to avoid the incorporation of air bubbles. When a clear mixture was obtained the batch was placed under a vacuum of 10 psi for a period of 1 hr, to be sure that the mixture was bubble-free. A portion of the mixture was then poured into a silicone mold (Fig. 1, M-2) representing the idealized molar with

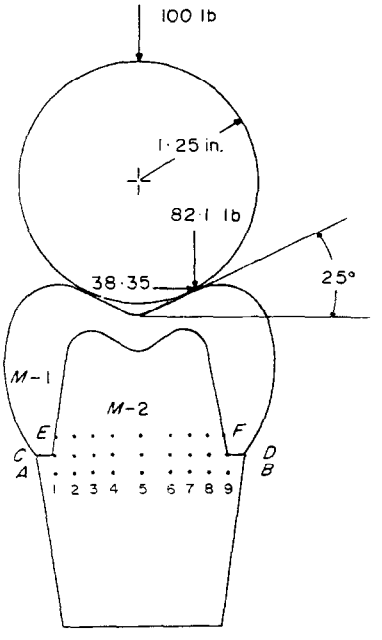

Fig. 1. Schematic of the axisymmetric composite tooth with 100 lb axisymmetric loading.

the full crown preparation, and it was allowed to polymerize for 3 days at room temperature. After this time the polymerized epoxy model was placed for 30 min in an oven at 140°F and then allowed to cool to room temperature. The above simulated the dentin in actual tooth. Another portion of the mixture was poured into a silicone mold (Fig. 1, M-1) representing the idealized gold crown casting and subjected to the following different curing cycle. After the 3-day polymerization the crowns were placed in the oven for 2 hr at 115°F and then permitted to cool to room temperature. Following this treatment the crowns were replaced in the oven at 212°F for 2 hr and again allowed to cool slowly to room temperature to avoid large thermal gradients. The restoration (M-1) as well as the tooth with the preparation (M-2) were then luted together using improved dental stone‡. For the stress-freezing process the photoelastic composite idealized tooth was placed in the oven for 1 hr at a constant temperature of 115°F, which allowed the tooth to reach a uniform temperature. The axisymmetric tooth was then loaded axisymmetrically with a 100 lb load. The temperature in the oven was held at 115°F for an additional hour. The heater of the oven was then shut off and the model allowed to cool to room temperature. Since the oven was well insulated the cooling was slow enough to avoid serious thermal gradients in the stress freezing range. Once the composite model was stress frozen it was sliced and the slices were polished and examined in a polariscope (Fig. 2).

B. *The finite element model*

The basic concept of the finite element method is the idealization of the actual continuum as an assemblage of a finite number of discrete structural elements, interconnected at a finite number of points or nodal points. The finite elements are formed by figuratively cutting the original continuum into a number of appropriately shaped sections, and retaining in the elements the properties of the original material. The analysis process consists of satisfying compatibility within

*Shell Chemical Co., Plastics & Resins Div., New York, New York, U.S.A.
†Jefferson Chemical Co., Austin, Texas, U.S.A.
‡Duroc, Ransom and Randolph Co., Toledo, Ohio, U.S.A.

each element, and equilibrium conditions at the nodal points. By concentrating the equivalent forces at the nodes, equilibrium conditions are satisfied in the overall sense only. Local violations of equilibrium conditions within each element and on its boundaries could arise. The finite element approach is in a sense, equivalent to the minimization of the total potential energy of the system in terms of a prescribed displacement field. If the displacement field is defined in a suitable way, then convergence to the correct value will occur. A computer program was written to evaluate the stresses in the axisymmetric model. The information needed for calculating the stresses is:

(1) total number of nodal points,
(2) total number of elements,
(3) a numbering system identifying each element,
(4) Young's modulus and Poisson's ratio associated with each element,
(5) a numbering system identifying each nodal point,
(6) the coordinates of each nodal point,
(7) the type of boundary constraints, and
(8) the evaluation of the forces at the external nodes.

Once these are specified, the displacements, as well as the stresses can be immediately calculated with the help of the program. The program was checked for the case of a thick-walled cylinder under internal pressure and the results of the stresses obtained by the finite element method agree remarkably well (Farah, 1972) with the theoretical values given by Timoshenko and Goodier (1951).

RESULTS

Ten photoelastic axisymmetric models were prepared as described earlier. Six of these models were loaded with a 50 lb load, two were loaded with a 70 lb load, and two were loaded with a 100 lb load. Nine averages of N, the fringe order which is directly proportional to the maximum shear stress given by

$$\tau_{max} = \frac{Nh}{2t} \tag{14}$$

were recorded in a central slice along lines A–B, C–D and E–F (Fig. 1) and the fringe order N along those lines are presented in tabular form in Table 1. The results for the axisymmetric model will be correlated with the ones obtained by the finite element method in the discussion.

The axisymmetric model was subdivided into 348 triangular elements and a number was assigned to each element as shown in Fig. 3. The axisymmetric model was loaded with an axisymmetric load of 100 lb which is assumed to be acting at node No. 3 and the model was assumed to be fixed at the base. The stresses at the centroid of each triangular element were calculated using the actual modulus and Poisson's ratio of gold and dentin, respectively, i.e. for gold $E = 13$ million psi and $\nu = 0{\cdot}33$, and for dentin $E = 2{\cdot}7$ million psi and $\nu = 0{\cdot}31$. Some of the results are presented in Table 2, where comparisons of maximum shear stresses by the photoelastic method and the finite element method are exhibited. In Table 3 the values of σ_r and σ_z along lines A–B through M–N are presented, and in Figs. 4 and 5 a plot was made of the variations along the radius of the axial stress (σ_z), as well as that of the radial stress (σ_r), along lines A–B, C–D, E–F, G–H, I–J, K–L and M–N as shown in Fig. 3.

DISCUSSION

Three-dimensional composite photoelastic studies have been limited because of the complexity involved in the determination of the complete state of stress in a three-dimensional irregularly shaped structure. In this study a simplification was introduced, i.e. the axisymmetric model, by which approximate yet reliable information could be acquired on the state of stress in the dental model. The justification of this simplifi-

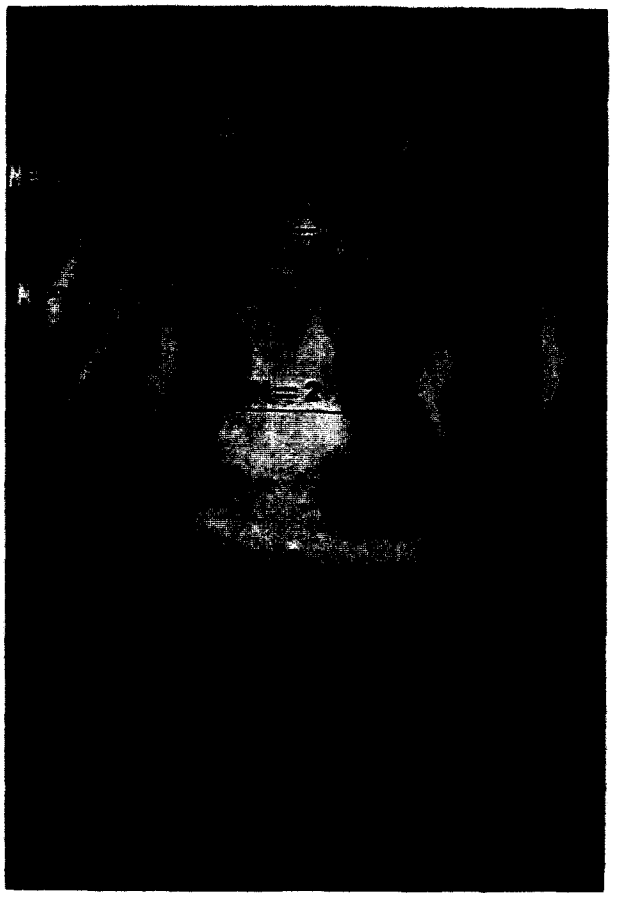

Fig. 2. Isochromatic stress pattern in the axisymmetric photoelastic model under 100 lb load.

(*Facing p.* 514)

Table 1. Average variations of N in a central slice of the axisymmetric model along lines $A-B$, $C-D$ and $E-F$

Location of N	Shoulder geometry Load = 50 lb N along lines $A-B$	$C-D$	$E-F$	Load = 70 lb N along lines $A-B$	$C-D$	$E-F$	Load = 100 lb N along lines $A-B$	$C-D$	$E-F$
1	1·66	2·54	0·00	2·62	3·12	0·14	3·35	3·60	0·73
2	1·18	1·07	0·82	1·56	1·52	1·02	2·33	2·04	1·76
3	1·14	1·14	1·05	1·44	1·46	1·36	2·23	2·23	2·13
4	1·19	1·21	1·17	1·48	1·52	1·50	2·33	2·40	2·37
5	1·25	1·27	1·27	1·51	1·48	1·56	2·46	2·52	2·56
6	1·19	1·21	1·17	1·48	1·52	1·50	2·33	2·40	2·37
7	1·14	1·14	1·05	1·44	1·46	1·36	2·23	2·23	2·13
8	1·18	1·07	0·82	1·56	1·52	1·02	2·33	2·04	1·76
9	1·66	2·54	0·00	2·62	3·12	0·14	3·35	3·60	0·73

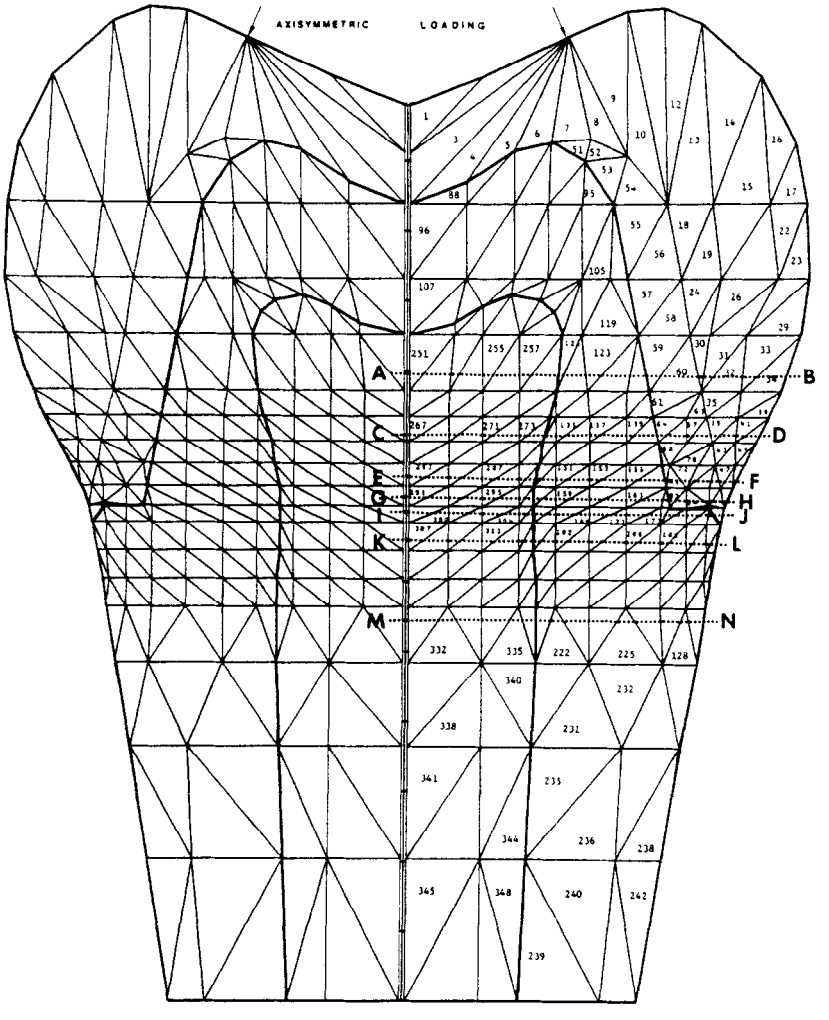

Fig. 3. Numbering order for the triangular finite elements of the axisymmetric model with the shoulder geometry.

Table 2. Variations of τ_{max} in the axisymmetric model along lines A–B, C–D and E–F, for the finite element and photoelastic method

Location (See Fig. 1)	Finite element Actual elastic constants	Photoelastic $\tau_{max} = \frac{Nf}{2h}$
Line A–B	τ_{max}-psi	τ_{max}-psi
5	10·50	12·80
6	10·20	12·20
7	9·95	11·81
8	10·31	11·28
9	12·60	13·32
Line C–D		
5	10·47	12·70
6	9·97	11·50
7	9·34	10·62
8	8·83	9·35
9	12·55	10·40
Line E–F		
5	11·35	12·95
6	10·56	11·30
7	9·43	9·56
8	8·26	8·56
9	7·27	6·35

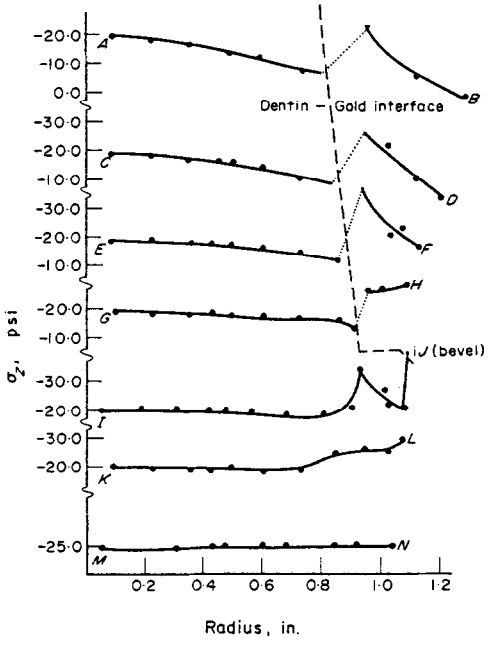

Fig. 4. Variations in the axial stresses, σ_z, as a function of the radius in the axisymmetric model along the specified lines.

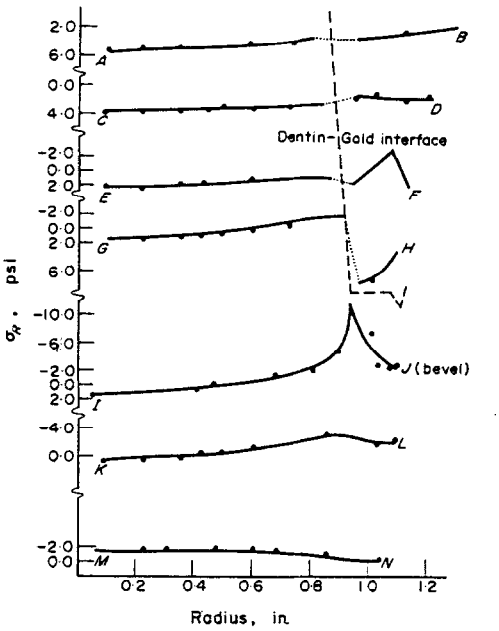

Fig. 5. Variations in the radial stresses, σ_r, as a function of the radius in the axisymmetric model along the specified lines.

cation is based upon some earlier work carried out by the authors (Farah and Craig, 1972) on actual composite photoelastic three-dimensional models. The dental models, representing the first molar, were constructed from the same photoelastic materials used in this study. These models were 5 times the size of an actual first molar. It was found, upon sectioning of the photoelastic models, that the shear stress distribution was fairly symmetrical on both sides of a plane passing through the middle of the molar.

Symmetry in the shear stress was also observed in slices taken along the long axis of the tooth. Also, upon checking Wheeler's *Atlas on Tooth Form* (1969) it was found that the dia. at the cervix measured mesio–distally or bucco–lingually was the same. Furthermore, the dia. of the crown of the mandibular first molar was again quite similar whether measured mesio–distally or bucco–lingually. The above observations led to the consideration of the axisymmetric approximation of the first molar.

Table 3. Radial and axial stresses as a function of the radius along the specified lines

Element No.	Line A–B R (in.)	σ_z (psi)	σ_r (psi)
252	0·11	−19·96	5·10
254	0·23	−18·83	5·06
256	0·36	−16·55	4·95
258	0·49	−13·96	4·78
122	0·60	−11·80	4·47
124	0·75	−7·71	4·16
125	0·82	−7·34	3·44
60	0·97	−21·83	3·55
32	1·14	−4·31	3·04
34	1·30	2·45	2·30

Element No.	Line C–D R (in.)	σ_z (psi)	σ_r (psi)
268	0·10	−19·18	3·59
270	0·23	−18·34	3·55
272	0·36	−17·02	3·42
274	0·46	−15·90	3·20
134	0·51	−15·33	2·94
136	0·61	−13·70	2·99
138	0·74	−10·62	2·95
140	0·85	−8·40	2·46
65	0·96	−25·12	1·69
67	1·04	−21·08	1·26
40	1·14	−9·56	2·27
42	1·22	−2·72	2·06

Element No.	Line E–F R (in.)	σ_z (psi)	σ_r (psi)
284	0·10	−19·11	1·12
286	0·23	−18·60	2·02
288	0·36	−17·72	1·84
290	0·44	−17·38	1·51
150	0·50	−16·76	1·33
152	0·61	−15·69	1·16
154	0·74	−13·96	0·97
156	0·87	−11·30	0·98
81	0·95	−36·34	1·73
74	1·05	−20·05	−1·74
75	1·09	−22·40	−2·84
48	1·14	−16·22	2·33

Element No.	Line G–H R (in.)	σ_z (psi)	σ_r (psi)
292	0·10	−19·24	1·53
294	0·23	−18·80	1·40
296	0·36	−18·08	1·18
298	0·43	−17·83	0·78
158	0·50	−17·35	0·55
160	0·61	−16·60	0·18
162	0·74	−15·62	−0·45
164	0·87	−16·00	−1·46
165	0·92	−12·70	−1·39
83	0·97	−25·71	7·54
84	1·02	−25·99	7·48
78	1·10	−27·42	3·38

Element No.	Line I–J R (in.)	σ_z (psi)	σ_r(psi)
299	0·06	−19·64	1·30
301	0·19	−19·45	1·05
303	0·31	−19·24	0·61
305	0·42	−18·58	0·39
166	0·48	−18·35	0·06
168	0·57	−18·10	−0·53
170	0·69	−17·77	−1·45
172	0·82	−17·57	−2·19
174	0·91	−20·49	−4·95
175	0·94	−33·24	−10·94
177	1·02	−26·78	−7·39
178	1·04	−21·77	−2·85
179	1·08	−20·24	−2·45
87	1·10	−39·10*	−2·60

*bevel

Element No.	Line K–L R (in.)	σ_z (psi)	σ_r (psi)
308	0·10	−19·91	0·49
310	0·23	−19·68	0·31
312	0·36	−19·09	0·14
314	0·43	−18·97	−0·24
181	0·50	−18·62	−0·45
183	0·61	−18·41	−0·96
185	0·64	−19·03	−1·71
187	0·86	−24·01	−2·86
189	0·96	−25·51	−2·29
191	1·04	−25·21	−1·83
193	1·09	−29·15	−1·91

Element No.	Line M–N R (in.)	σ_z (psi)	σ_r (psi)
331	0·06	−24·54	−1·65
333	0·23	−23·79	−1·35
334	0·31	−23·95	−1·64
336	0·44	−24·60	−1·62
221	0·48	−24·73	−1·89
223	0·61	−24·15	−1·78
224	0·69	−24·14	−1·72
226	0·86	−24·91	−1·02
227	0·93	−24·54	−0·37
229	1·03	−23·93	−0·25

Ten photoelastic axisymmetric models were prepared and axisymmetrically loaded. The fringe order N along lines A–B, C–D and E–F were tabulated in Table 1 for three different loads. From Table 1 the linear behavior of the epoxy resin can be observed, at twice the load most values of N at 100 lb load were twice those at 50 lb load.

In Table 2 the variations of τ_{max} in the axisymmetric model along lines A–B, C–D and E–F were presented for both the finite element and the photoelastic method. It can be seen that the maximum shear stresses obtained by the finite element method for $E_{gold} = 13{,}000{,}000$ psi, $\nu = 0{\cdot}33$ and $E_{dentin} = 2{,}700{,}000$ psi, $\nu = 0{\cdot}31$ compared favorably to those obtained by the photoelastic method. For example, τ_{max} along line C–D, location 7 had a value of 9·34 psi in the finite element model, and 10·62 psi in the photoelastic model. The shear stresses obtained photoelastically were generally somewhat higher than those obtained by the finite element method. It is believed that this was partly a result of the more rigid conditions imposed at the dentin and gold interface by the finite element method. When using the finite element method it was assumed that the gold and the dentin were firmly bonded; this was a necessary assumption because continuity at the boundary had to be satisfied. But in actuality, i.e. in the case of the photoelastic model, bonding was hardly the case since the dental stone used to lute the crown to the preparation functioned more as a buffer zone than a cement. The conditions at the dentin and gold interface, therefore, were more lax in the case of the actual photoelastic model. Consequently, the shear stresses in the crown were bound to be of a higher magnitude. The conditions at the interface could have been more closely approximated in the idealized model (finite element treatment), by assuming that small springs connected the crown to the preparation. By varying the stiffnesses of these springs one could conceivably approach the actual situation at the gold to dentin boundary.

In order to obtain a more detailed picture of the stress distribution in the axisymmetric model a plot of the axial and radial stresses were made (Figs. 4 and 5) along specified lines shown in Fig. 3. In Fig. 4 the axial stress (σ_z) was plotted as a function of the radius. Along lines A–B, C–D, E–F and G–H it can be seen that the stress, σ_z, decreased uniformly in the dentin from the center of the tooth to the dentin–gold interface where a sudden increase in σ_z occurred in the restoration. The increase in σ_z would be expected because of the higher modulus of the gold. On line I–J the effect of the gold crown was still sharply exhibited by the sudden increase in σ_z immediately under the shoulder. A more gradual effect was observed along line K–L and as one moved further away from the effects of the marginal change the stress became more and more uniform throughout the dentin as shown in line M–N.

The same type of observations can be drawn from Fig. 5, where the radial stress as a function of the radius was plotted. In this case the discontinuity across the dentin–gold interface was of a lesser magnitude, as expected, since equilibrium had to be satisfied in the radial direction. As would be expected, as the size of the elements decreased in the immediate vicinity of the dentin–gold interface the radial stress on both sides of the margin should converge to one value.

An exception was observed in line G–H where the radial stress was quite different at the dentin–gold interface. This exception is a result of the close proximity of line G–H to the shoulder, i.e. right angle geometry. It is interesting to note the change in the radial stress from tension to compression in areas near the shoulder, and it is believed that smaller subdivisions of the elements in that area would be necessary to obtain a

precise measure of stress. The magnitude, as well as the direction, of the stress at the dentin–gold interface is of great interest since knowledge of these could shed some light on the kind of cement to be used, or the reason why failure might occur at the junction.

In this study, the finite element method proved to be a useful tool for analyzing a dental model. The finite element method has the advantage of providing information about the complete state of stress in a body. By contrast the photoelastic method gives limited direct information, i.e. the maximum shear stress, and separation methods must be used to obtain the other components of the stress tensor. Unfortunately, these methods such as the shear difference method are time consuming and require a great amount of care.

CONCLUSION

The use of an axisymmetric model proved to be a sound approach for obtaining approximate yet reliable information concerning the stress distribution in a tooth. The photoelastic approach provides a clear visual and qualitative picture of the stress distribution for the applied scientist, whereas the finite element approach provides a more detailed evaluation of the complete state of stress in the model for the researcher. The combination of the above methods permits a better understanding of the stress distribution in dental restorations as a result of the forces of mastication.

Acknowledgement—This investigation was supported by USPHS Research Grant DE-01817 from the National Institute of Dental Research, Bethesda, Maryland.

REFERENCES

Argyris, J. H. (1965) Matrix analysis of three-dimensional elastic media for small and large deflection. *AIAA J.* **3**(1), 45–51.

Argyris, J. H. and Redshaw, J. C. (1968) Three-dimensional analysis of two arch dams by a finite element method. *Proc. Symp. Arch. Dams, Inst. Civ. Eng.*

Clough, R. W. (1960) The finite element method in plane stress analysis. *Proc. 2nd ASCE Conf. on Electronic Computation*, Pittsburgh, Pa., Sept.

Clough, R. W. and Wilson, E. C. (1963) Stress analysis of a gravity dam by the finite element method. RILEM Bull., No. 19, June.

Colin, L., Kaufman, E. G. and Paprino, R. (1963) Stress concentrations in full crown preparations. *N. Y. State Dent. J.* **29**, 370–373.

Craig, R. G., El-Ebrashi, M. K., LePeak, P. J. and Peyton, F. A. (1967a) Experimental stress analysis of dental restorations—I. Two-dimensional photoelastic stress analysis of inlays. *J. Prosth. Dent.* **17**, 277–291.

Craig, R. G., El-Ebrashi, M. K. and Peyton, F. A. (1967b) Experimental stress analysis of dental restorations—II. Two-dimensional photoelastic stress analysis of crowns. *J. Prosth. Dent.* **17**, 292–302.

El-Ebrashi, M. K., Craig, R. G. and Peyton, F. A. (1969a) Experimental stress analysis of dental restorations—III. The concept of the geometry of proximal margins. *J. Prosth. Dent.* **22**, 333–345.

El-Ebrashi, M. K., Craig, R. G. and Peyton, F. A. (1969b) Experimental stress analysis of dental restorations—IV. The concept of parallelism of axial walls. *J. Prosth. Dent.* **22**, 346–353.

El-Ebrashi, M. K., Craig, R. G. and Peyton, F. A. (1969c) Experimental stress analysis of dental restorations—V. The concept of occlusal reduction and pins. *J. Prosth. Dent.* **22**, 565–577.

El-Ebrashi, M. K., Craig, R. G. and Peyton, F. A. (1969d) Experimental stress analysis of dental restorations—VI. The concept of proximal reduction in compound restoration. *J. Prosth. Dent.* **22**, 663–670.

El-Ebrashi, M. K., Craig, R. G. and Peyton, F. A. (1970) Experimental stress analysis of dental restorations—VII. Structural design and stress analysis of fixed partial dentures, *J. Prosth. Dent.* **23**, 177–186.

Ergatoudis, J., Irous, B. M. and Zienkiewicz, O. C. (1968) Three-dimentional analysis of arch dams and their foundations. *Proc. Symp. Arch. Dams, Inst. Civ. Eng.*

Farah, J. W. (1972) Stress analysis of first molars with full-crown preparations by three dimensional photoelasticity and the finite element method. Ann Arbor, The University of Michigan, Doctoral Dissertation, 124 p.

Farah, J. W. and Craig, R. G. (1972) Three-dimensional photoelastic stress analysis of first molars with full-crown preparations. Presented at the *50th Annual Meeting of the International Association for Dental Research*, Las Vegas.

Grafton, P. E. and Strome, D. R. (1963) Analysis of axisymmetric shells by the direct stiffness method. *AIAA J.* **1**, 2342–2347.

Haskins, R. C., Haack, D. C. and Ireland, R. L. (1954) A study of stress pattern variation in class I cavity restorations as a result of different cavity designs. *J. Dent. Res.* **33**, 757–766.

Johnson, E. W. (1965) A three-dimensional photoelastic investigation of stress concentrations in operably deformed human teeth. Edmonton, University of Alberta, School of Engineering, Thesis, 89 p.

Johnson, E. W., Castaldi, C. R., Gau, D. J. and Wysocki,

G. P. (1968) Stress pattern variations in operatively prepared human teeth, studied by three-dimensional photoelasticity. *J. Dent. Res.* **47**, 548–558.

Lehman, M. L. and Hampson, E. L. (1962) A study of strain patterns in jacket crowns on anterior teeth resulting from different tooth preparations. *Brit. Dent. J.* **113**, 337–345.

Mahler, D. B. and Peyton, F. A. (1955) Photoelasticity as a research technique for analyzing stresses in dental structures. *J. Dent. Res.* **34**, 831–838.

Mahler, D. B. (1956) A photoelastic analysis of the stresses developed in a restored primary tooth when subject to forces of mastication. Ann Arbor, The University of Michigan, Doctoral Dissertation, 129 p.

Noonan, M. A. (1949) The use of photoelasticity in a study of cavity preparations. *J. Dent. Child.* **16**, 24–28.

Ping, T. and Pian, T. H. H. (1967) The convergence of finite element method in solving linear elastic problems. *Int. J. Solids Struct.* **3**, 865–880.

Rashid, Y. R. and Rockenhauser, W. (1968) Pressure vessel analysis by finite element techniques. *Proc., Conferences on Prestressed Concrete Pressure Vessels, Inst. Civ. Eng.*

Timoshenko, S. and Goodier, J. N. (1951) *Theory of Elasticity*, p. 60. McGraw-Hill, New York.

Turner, M. J., Clough, R. W., Martin, H. C. and Top, L. J. (1956) Stiffness and deflection analysis of complex structures. *J. Aero. Sci.* Sept. 23.

Walton, C. B. and Leven, M. M. (1955) A preliminar report of photoelastic tests of strain patterns within jacket crowns. *Am. Dent. A. J.* **50**, 44–48.

Wheeler, R. C. (1969) *An Atlas of Tooth Form.* Saunders, Philadelphia.

Zienkiewicz, O. C. (1971) *The Finite Element Method in Engineering Science*, Chap. 5. MacGraw-Hill, New York.

NOMENCLATURE

E	Young's Modulus (modulus of elasticity)
f	stress optical coefficient
h	thickness
N	integer, order of extinction, number of fringes
r	radial coordinate
z	axial coordinate
ν	Poisson's ratio
σ_r, σ_z	normal stress in the r, and z direction
τ_{max}	maximum shear stress.